

# ULTRASTRUCTURE OF SOME OSTRACODS

NIELS OLUF JØRGENSEN

JØRGENSEN, N. O.: Ultrastructure of some ostracods. *Bull. geol. Soc. Denmark*, vol. 20, pp. 79-92. Copenhagen, July 9th, 1970.

The ultrastructure of the valves of five recent species of ostracods is investigated. These are *Cypreideis* sp., *Bythocypris* sp., *Xestoleberis* sp., *Cythereis* sp. and *Trachyleberis dunelmensis* (Normann, 1865).

In order to determine the orientation of the crystalline matter the valves were studied in polarized light and in an X-ray diffractometer. The results indicate that the crystals are extremely well orientated with the optical axes perpendicular to the shell surface.

All the sections studied in the transmission electron microscope show that the ostracod valve is built of small crystal units enclosed by organic membranes. The diameter of the crystal units generally is about  $2\mu$ . The crystal units generally show no preferred morphological orientation.

Besides the calcite the ostracod valve consists of organic matter in form of a matrix. Organic sheets form a part of the matrix and lie parallel or subparallel to the valve surface. The sheets do not extend the full length of the valve, but continue only for a shorter distance.

The morphology of the pore canals is investigated in the scanning electron microscope. The normal pore canals have a very variable construction in the species studied, while the marginal pore canals appear to enclose only the penetrating setae.

The fundamental study of the structure of the ostracod valves was published by Müller (1894). He determined the chemical composition to be  $\text{CaCO}_3$  and  $\text{MgCO}_3$ , and by using a polarizing microscope the calcareous matter was found to have an amorphous or fine-grained structure. In a few instances he observed calcite prisms orientated perpendicular to the wall surface. By staining methods he demonstrated the presence of an outer and inner chitinous layer, and organic material inside the calcareous part of the valve.

Schmidt (1924) and Dudich (1929, 1931) dealt with the optical habits of the calcareous matter and found by use of the polarizing microscope an extinction which indicated an orientation of the optical axes perpendicular to the wall surface. Porkorny (1952) observed an organic framework in the valves of Pliocene material.

Chave (1954) investigated the chemical composition of the ostracod

valve by X-ray diffraction and found it to be  $\text{CaCO}_3$  with 0–10 % content of  $\text{MgCO}_3$ . He suggested a positive linear correlation between the Mg content and the water temperature of the biotope.

Harding (1964) investigated sections of the carapace by staining methods with special reference to the hinge and the shell margin.

## Material

In the present investigation five recent species are studied. These are *Cypreideis* sp. and *Bythocypris* sp. taken from the eastern part of the Mediterranean, and *Xestoleberis* sp., *Cythereis* sp. and *Trachyleberis dunelmensis* (Normann, 1865) which were recently collected from the Kattegat.

Morphologically they range from unornamented to reticulate and strongly ornamented forms.

Systematically they represent four different subfamilies in the suborder Podocopina, which is the most important suborder.

## Light-microscopical observations

Whole valves, crushed specimens and thin sections orientated at right angles to the shell surface were studied under the light microscope between crossed nicols.

All the specimens studied showed organized extinction parallel to the polarizing directions of the nicols (pl. 1, figs 1–2). This phenomenon was earlier described by Schmidt (1924) and Dudich (1931) within the Ostracoda and thoroughly discussed by Wood (1949) within the Foraminifera. From the light-microscopical investigations the orientation of the c-axes of the calcite crystals thus appears to be perpendicular to the shell surface. This feature is most clearly seen in the unornamented valves. Reticulate or strongly ornamented specimens show only a diffuse extinction.

The small distinct black crosses observed by Schmidt (1924, p. 263, fig. 135 a-b) in reticulate valves would seem to be air bubbles trapped in pits in the reticulated valve surface.

## X-ray diffraction investigations

In order to obtain more conclusive information as to the orientation of the crystalline matter of the ostracod valve the X-ray diffraction technique earlier used within foraminifera by Hansen (1968) was applied.

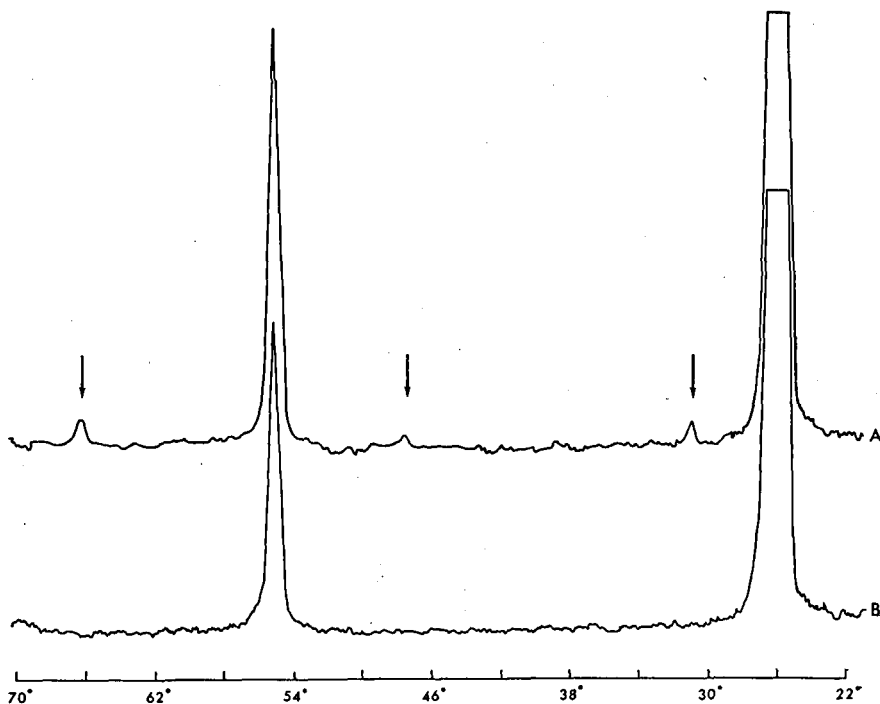


Fig. 1. A. The diffraction curve obtained from *Xestoleberis* sp. The arrows point to the three observed calcite peaks. B. The diffraction curve obtained from the clean quartz plate.

Specimens of the unornamented *Xestoleberis* sp. recently sampled in the Kattegat were used to get flat pieces of valves.

The valves were crushed between two glass plates and small flat pieces were selected and mounted with gum tragantum on a quartz plate.

The samples were run in a Phillips X-ray diffractometer with Cu K $\alpha$ -radiation selected by a curved crystal NaF monochromator. The beam width was 1° and a proportional counter was used.

The quartz plate was used as it gave a very low background and only few well-defined reflexes not coinciding with the calcite peaks.

In fig. 1. is shown the diffraction curve obtained from *Xestoleberis* sp. together with the curve from the quartz plate for comparison.

For identification of the reflexes the ASTM catalogue no. 5-0586 was used.

Further comparison was made with the reflection intensities obtained from a non-orientated calcite powder.

Table 1. Comparison between the xray diffraction results from *Xestoleberis* sp. and a non-orientated calcite powder

hkil	dÅ	2θ	A	B	C
10 $\bar{1}$ 2	3.8600	22.7	20	0	16.0
10 $\bar{1}$ 4	3.0354	29.4	1690	0	1352
0006	2.8465	31.4	6.5	5.2	5.2
11 $\bar{2}$ 0	2.4926	36.0	39	0	31.2
11 $\bar{2}$ 3	2.2850	39.4	45	0	36.0
20 $\bar{2}$ 2	2.0924	43.2	54	0	43.2
10 $\bar{1}$ 8	1.9125	47.5	130	2.6	104
11 $\bar{2}$ 6	1.8754	48.5	40	0	32.0
21 $\bar{3}$ 1	1.6300	56.4	9	0	7.2
21 $\bar{3}$ 2	1.6040	57.4	17	0	13.6
10 $\bar{1}$ .10	1.5863	58.1	3	0	2.4
20 $\bar{2}$ 8	1.5405	60.0	39	0	31.2
21 $\bar{3}$ 4	1.5244	60.7			
11 $\bar{2}$ 9	1.5087	61.4			
21 $\bar{3}$ 5	1.4703	62.9	5.5	0	4.4
30 $\bar{3}$ 0	1.4395	64.7	16	0	12.8
000.12	1.4219	65.6	12	6.0	9.6

Column A shows the intensities recorded in counts per second from the non-orientated calcite powder.

Column B shows the intensities recorded in counts per second from *Xestoleberis* sp. Column C shows the intensities to be expected from B if *Xestoleberis* sp. had been built of randomly orientated calcite crystals, and if (0006) had the same intensity per gram in the specimen A and B.

The values of reflection intensities are listed in table 1.

The peak at  $2\theta = 31^\circ.4$  corresponds to the reflection from the basal pinacoid (0006) in the structural setting of Bragg (1914). The peak at  $2\theta = 47^\circ.5$  is the reflection from the rombohedron (10 $\bar{1}$ 8) and that of the second order basal pinacoid (000.12) is found at  $2\theta = 65^\circ.6$ .

It is highly remarkable that the reflection from the cleavage rombohedron (10 $\bar{1}$ 4)  $2\theta = 29^\circ.4$  cannot be distinguished from the low background. By contrast the reflections from the basal pinacoid (0006) and (000.12) as well as the rombohedron (10 $\bar{1}$ 8) are distinct. These reflexes indicate that the basal pinacoid of the calcite crystals is extremely well orientated parallel

to the surface of the wall. This corroborates the observations from the light microscope.

The presence of the reflection from  $(10\bar{1}8)$  is most likely due to the fact that the fragments of the valves are not perfectly plane (Hansen, 1968).

## Technique

For the studies of ultrastructures longitudinal, transverse and tangential sections were studied both in transmission electron microscope and in scanning electron microscope. In the following the two types of electron microscopes are termed TEM and SEM respectively.

The technique described by Hansen (1967) was applied for preparation of the sections for the TEM. The ostracod valve or carapace was embedded in araldit and ground with frosted glass plates to the desired level. It was polished with MgO-powder to remove the grinding tracks.

The section was etched with a saturated aqueous solution of EDTA (EDTA = ethylene-diamin-tetra-acetate) for 10–20 seconds and afterwards washed in distilled water.

The dry section was replicated using collodium dissolved in amylacetate. The stripped replica was washed in 10 % HCl to remove possible calcite crystals which it may have pulled out. The replica was then washed in distilled water, dried and shadowed with carbon in a vacuum evaporator. To avoid empty shadows the replica was shaded in two opposite directions in the ratio 1:3. The thickness of the carbon film was about 200 Å. Transfer of the shadowed replica to cut-out grid has been described by Hansen (1967).

In general the first replica after etching showed a high concentration of organic material. After several replications the sections were rather clean. It is, however, very difficult to remove the organic material completely by replication.

A special method for study of organic material has been described by Hansen (1970). The etched section proper was shadowed with carbon and replicated with collodium. The replica was stripped carefully contemporary with dissolution of the specimen in 10 % HCl. The organic material stuck to the replica which was transferred to a grid and dissolved in a reflux-unit. In a variant the replica with the organic material was shadowed after stripping.

For investigation of the organic material in the SEM broken valves were mounted on a specimen-stub by use of pandeticon glue diluted by acetone. The valves were then etched in an EDTA-solution for one hour. The specimens were washed in distilled water for 2–3 hours. They were dried and

plated with 200 Å gold while rotating in a vacuum evaporator (Hay & Sandberg, 1967).

### The crystal units

In all the sections studied it was observed that the ostracod valve is built of small crystal units each enclosed by organic membranes.

The diameter of the crystal units generally is about 2  $\mu$ . Within a section the diameter normally ranges from 0.5  $\mu$  to about 6  $\mu$ .

In the unornamented forms smaller and larger crystal units occur together and are generally not distributed according to size (pl. 1, fig. 3).

A problematical exception to this was found in only one section of *Xestoleberis* sp. where a distinct difference in crystal unit size in the outer and inner lamella could be observed (pl. 2, fig. 3). In the inner lamella the diameter of the units is from 0.5–1  $\mu$  whereas it is 2–3  $\mu$  in the outer lamella. The boundary between the two lamellae is distinct. The different sizes of the crystal units are only met within the marginal zone. Among the 22 sections made of *Xestoleberis* sp. only the one figured here showed different distribution of crystal sizes while the remaining sections all demonstrated the irregular distribution of crystal units of different diameter.

Specimens of *Trachyleberis dunelmensis* were used as representative of the strongly ornamented species. The ornamentation of this species is composed of reticulation as well as spines.

In tangential sections the centre of the proximal part of the spines was found to be built of relatively few larger crystal units with a diameter of about 5  $\mu$  (pl. 3, fig. 2). In the distal part of the spines smaller crystal units with a diameter of about 2  $\mu$  were found as in the wall of the unornamented valves (pl. 3, fig. 1). The larger crystal units in the interior of the proximal part of the spines interfinger with the smaller crystal units in the exterior. The presence of larger crystal units in the central basal part of the spines is confined to the spines and is not found in the reticulation or the inner part of the shell.

In sections of both ornamented and unornamented valves the crystal units were seen to be variable in outline, changing from angular to somewhat rounded, indicative of subhedral crystals (pl. 2, figs 1–2).

The micrographs shown in the present work reveal that the crystal units generally show no morphological orientation. In view of the optical orientation of the mineral matter of the valves the general lack of morphological orientation appears striking. In some cases areas with slight elongation of the crystal units in the direction parallel or subparallel with the surface of the valve have been observed (pl. 3, figs 1–2).

## The organic matrix

Besides calcite the ostracod valve consists of organic matter constituting a matrix. The matrix is limited by an inner and outer organic layer (pl. 5, fig. 4). By removing the calcite the organic matrix is found to resemble a three-dimensional spongy framework (pl. 4, fig. 2). In the cavities of this framework single calcite crystals are found. The enclosing membranes appear in sections as black frayed bands in the boundaries between the crystal units (pl. 2, fig. 1). The organic material has been torn out while stripping the replica. Some times the membranes are collapsed while in other instances they remain erect and cause shadows.

A close examination of the membranes reveals that they are riddled by perforations of an order of magnitude of  $0.1 \mu$  (pl. 4, fig. 1).

In all longitudinal and transverse sections sheet-like concentrations of organic material were found orientated parallel or subparallel with the valve surface (pl. 1, fig. 3; pl. 2, fig. 3). The sheets are readily distinguished from the membranes enclosing the crystal units by their regularity and higher concentration of material. They do not extend the full length of the shell. Distance up to two thirds of the length or height of the valve have been observed, but in general they continue only for a shorter distance.

The distribution of organic sheets within the investigated species shows no regularity. They are found both close to inner as well as outer surfaces and in the middle of the shell.

## Pore canals

The pore canals of the five species have been studied. In addition to the surface replicas for the TEM, inner and outer surfaces and broken valves were investigated in the SEM.

The normal pore canals of *Xestoleberis* sp. are slightly funnel-shaped. They consist of up to about 100 small cylindrical organic tubes penetrating the valve in a cluster (pl. 5, fig. 1). The diameter of the single small tubes is about  $0.3\text{--}0.5 \mu$ . The outer openings of the tubes are situated in an organic pore plate placed just below the level of the surface. The outline of the pore plate is circular with a diameter of about  $12 \mu$ . A seta penetrates the centre (pl. 5, fig. 2). The pore terminates internally in a rounded depression.

In the strongly ornamented *Trachyleberis dunelmensis* the normal pore canals run along the centre of the spines or in some instances penetrate the distal part of the spine wall (pl. 5, fig. 3). No internal pore plate has been observed in this species. The diameter of the pore canal is about  $5 \mu$ .

The normal pore canal of *Cythereis* sp. consists of a thickwalled organic pore tube, widening in the proximal part and with an average diameter of

about 10  $\mu$  (pl. 6, fig. 1). About one quarter of the way from the outer opening is found a perforated organic pore plate with a thickness of 1–1.5  $\mu$ . The perforations in the pore plate have a diameter of 0.2–0.5  $\mu$ . The pore canal is provided with a seta which penetrates the pore plate in the centre (pl. 6, fig. 2.).

The outer third of the normal pore canal in *Cypredeis* sp. consists of small organic tubes while the inner two-thirds is a narrow pipe widening towards the proximal part and enclosing the seta (pl. 6, fig. 4). The outline of the outer pore plate varies in the same specimen from subcircular to elongate or slitlike (pl. 6, fig. 3). The order of magnitude of the longest diameter is 10–20  $\mu$ . The seta is not necessarily placed in the centre of the pore plate but may also be found in the margin of the pore plate.

The normal pore canal of *Bythocypris* sp. consists of a narrow pore tube with a diameter of 1–2  $\mu$ . In the distal part, just inside the outer surface, is a widening of the pore canal forming a cavity filled with a spongy material (pl. 7, fig. 1). The diameter of the cavity is about 4  $\mu$ . The outer opening of the pore is a single pore aperture with a diameter of about 0.5  $\mu$  (pl. 7, fig. 2). The pore canals in the specimens of *Bythocypris* sp. studied by the present author contained no setae.

The marginal pore canals consist in all species studied of simple organic tubes enclosing a penetrating seta (pl. 7, figs 3–4). Pore plates were not found in any of the species studied.

## Discussion and conclusions

Müller (1894) showed the presence of a chitinous matter in the calcareous part of the valve. He suggested that it penetrated to different depths of the valve from the outer chitinous layer. Sometimes it had a concentric appearance, sometimes as sheets parallel to the valve surface or beams perpendicular to this direction. He also found a structure explained by him as a chitinous framework.

The present investigation shows that the organic matrix has an equal distribution throughout the valve and does not have any preferred connection to the outer organic layer. The only concentration of organic material is found in the sheets and the pore canals.

Richards (1958) showed by investigations of the arthropod cuticle that the endocuticle contains chitin, while the epicuticle contains protein but lacks chitin.

The general classification of the ostracods deals with two different kinds of normal pore canals; The normal pore canal and the sieve-type normal pore canal (Müller 1894, Porkorny 1958 and Morkhoven 1962).



Moore (1961, p. 53) defined the normal pore canal as: "Tubule piercing approximately at right angle almost any part of valve, commonly with enlarged proximal part lined with chitin; in living ostracods carries hair (seta) that projects from the surface."

The sieve-type pore canal he defined as: "Wide normal pore canal partially closed by an internal apparently perforate plate." (1961, p. 55).

Müller (1894) stated that the small perforations in the sieve-type normal pore canal were sealed at the distal part only leaving a central hole as pore aperture. He suggested their possible function as light-sensitive organs.

Triebel (1941, 1950, 1956) showed, however, sieve-type normal pore canals with fully perforated outer pore plate.

The first study of the outer morphology of the normal pore canals by use of scanning electron microscope was published by Sandberg & Plusquellec (1969). They investigated several genera and found a wide variation especially in the sieve-type normal pores. They showed that both the simple pore canals and the sieve-type normal pore canals are present in the two families Trachyleberididae and Hemicytheridae. The two pore types may even coexist in the same specimen.

Their scanning micrograph showing the outer pore plate in *Xestoleberis* sp. agrees well with the structure found by the present author (pl. 5 fig. 2).

The five species investigated by the author show that the normal pore canals are somewhat differently constructed. The marginal pore canals, on the other hand, seem to be simple penetrations for setae.

The few demonstrated examples show that the pore canals as a taxonomic feature need more intensive study.

Travis (1963) suggested a model of calcification of the decapod exoskeleton. She divided the cuticle into epi- exo- and endocuticle and a membraneous layer in intimate contact with the epidermis, calcification taking place in the exo- and endocuticle. The process begins in the already completed matrix of the exocuticle, while it is simultaneous with the formation of the new endocuticle. It was suggested that the process is under the control of the epidermal cells. One of the reasons of this was the presence of "pore canals" (protoplasmic extensions of the epidermis) which penetrate at right angles to the cuticle. The diameter of the "pore canals" ranges from  $0.5 \mu$  near the cell surface to  $0.1 \mu$  near the epi- exocuticle junction. The distribution of these "pore canals" is very dense.

It is evident that this model of calcification cannot be applied in the case of the ostracod valve. There is no differentiation in the calcareous part of the cuticle and more important, no "pore canals" as described by Travis. In addition, the size of the mineralized "bricks" found by Travis ranges from  $500 \text{ \AA}$  to about  $0.2 \mu$ , while the crystal units in the ostracod valve are found to have a diameter of about  $2 \mu$ .

Travis also investigated the crystalline  $\text{CaCO}_3$  by use of X-ray diffraction but did not find any preferred crystallographic orientation. This is contrary to the extremely good crystallographic orientation of the crystal units of the ostracod valve demonstrated by the present author.

The ultrastructure of the ostracod valve can be characterized as a three-dimensional organic framework limited by an outer epicuticle and an inner non-calcified part of the endocuticle. The organic sheets and the pore canals form an integral part of the organic matrix.

After the formation of the organic matter the calcite has been precipitated. The organic matrix has inhibited the natural growth of the crystals and determined their subhedral shape.

There is no evidence of secondary growth either in the outer (*viz.* the ornamentation) or in the inner part of the valve. The final shape of the valve was completed by the formation of the organic matrix prior to calcification.

Moss (1964) gave a general theory of calcification also with reference to the orientated crystal growth. He suggested the presence of a primarily organic matrix, which consists of two components: An organized active phase and an unorganized phase termed "ground substance". The calcification has taken place after the completion of the organic matrix. The orientated calcification is initiated by epitaxi. The organized component of the matrix is considered to interduce the first unit cells of the inorganic phase, and be capable of determining the crystallographic axes of the substance.

The latest discussions of biological calcification have been published by Towe & Cifelli (1967) and Degens (1967).

The present observations of the ostracod valve are in good agreement to this general theory of biological calcification. More intensive investigations, however, are needed to work out a specific calcification model of the ostracod valve, also with reference to the relationship between the calcareous and the soft parts.

*Acknowledgements.* The author is indebted to the staff of the Geological Institutes of the University of Copenhagen; for valuable help and advice the author is especially indebted to mag. scient. H. J. Hansen.

A special thank is given to mr. E. Gerry for placing material at the authors disposal. Dr. R. G. Bromley kindly improved the English manuscript.

## Dansk sammendrag

Den ultrastrukturelle opbygning af calcitskallerne er undersøgt hos fem recente ostracod-arter: *Cypreideis* sp., *Bythocypris* sp., *Xestoleberis* sp., *Cythereis* sp. og *Trachyleberis dunelmensis* (Normann, 1865).

Den optiske orientering af calcitkrystallernes c-akser er ved hjælp af polarisationsmikroskop og røntgen-diffraktometer bestemt til at være vinkelret på skaloverfladen.

Undersøgelse af længde-, tvær- og tangentialsnit i transmission elektron mikroskop viser at skallen er opbygget af små krystalenheder i størrelsesordenen 2  $\mu$ . Krystalenhederne har almindeligvis ingen foretrukken morfologisk orientering.

Foruden af calcit består ostracodskallen af en organisk matrix, som omgiver hver enkelt krystalenhed. De organiske vægge er et fremtrædende element i den organiske matrix. De forløber parallelt med skaloverfladen, men har ikke i noget tilfælde kunnet følges i hele skallens længde eller højde.

Porekanalernes opbygning hos de fem ostracod arter er undersøgt i scanning elektron mikroskop. De normale porekanaler udviser en meget varieret morfologi fra art til art, mens marginalporene kun synes at være udtrædelsessted for setae.

*Institut for historisk Geologi og Palæontologi  
Østervoldgade 5, DK-1350 København K, Denmark  
January 27th, 1970*

## References

- Bragg, W. L. 1914: The reflections of x-ray by crystals. *Proc. Roy. Soc. London*, **89A**, 246 only.
- Bragg, W. L. 1914: The analysis of the crystals by the x-ray spectrometer. *Proc. Roy. Soc. London*, **89A**, 468 only.
- Chave, K. E. 1954: Aspects of the biochemistry of the magnesium. 1. Calcareous marine organisms. *Journ. Geol.* **62**, 266–283.
- Degens, E. T. 1967: Evolutionary trends inferred from the organic tissue variation of mollusc shells. *Meddr dansk geol. Foren.* **17**, 112–124.
- Dudich, E. 1929: Die Kalkeinlagerungen des Crustaceenpanzers in polarisiertem Licht. *Zool. Anz.* **85**, 257–264.
- Dudich, E. 1931: Systematische und biologische untersuchungen über die Kalkeinlagerungen des Crustaceenpanzers in polarisiertem Licht. *Zoologica Stuttg.* **30**, 80, 1–154.
- Hansen, H. J. 1967: A technique for depiction of grind sections of foraminifera by aid of compiled electronmicrographs. *Meddr dansk geol. Foren.* **17**, 128–129.
- Hansen, H. J. 1968: X-ray diffractometer investigations of a radiate and a granulate foraminifera. *Meddr dansk geol. Foren.* **18**, 345–348.
- Hansen, H. J. (in press): Electron-microscopical studies on the ultrastructures of some calcite radiate and granulate foraminifera. *Biol. Skr. Dan. Vid. Selsk.*
- Harding, J. P. 1964: Crustacean cuticle with reference to the ostracod carapace. *Pubbl. Staz. Zool. Napoli* **33**, 9–29.
- Hay, W. W. H. & Sanberg, P. A. 1967: The scanning electron microscope, a major break-through for the micropaleontology. *Micropaleontology* **13**, 407–418.
- Moore, R. C. 1961: Glossary of the morphological terms applied to Ostracoda. *Treatise on Invertebrate Paleontology Q*, 47–56.

- Morkhoven, F. P. C. M. van. 1962: *Post-Palaeozoic Ostracoda. Their morphology, taxonomy and economic use. General.* 204 pp. New York: Elsevier Publishing Company.
- Moss, M. L. 1964: The phylogony of mineralized tissue. *International Review of general and experimental Zoology* **1**, 297-331.
- Müller, G. W. 1894: Die Ostracoden des Golfes von Neapel und der angrenzenden Meeresabschnitte. *Fauna und Flora des Golfes von Neapel*, 1-404. Berlin.
- Porkorny, V. 1952: The ostracods of the so-called Basal Horizon of the Subglobosa beds at Hodonin (Pliocene, Inner Alpine Basin Czechoslovakia). *Sbornik UUG* **19**, odd. pal., 229-396.
- Porkorny, V. 1958: *Grundzüge der Zoologischen Mikropaläontologie, II.* 453 pp. Berlin: DVW.
- Richards, A. G. 1958: The cuticle of Arthropoda. *Ergebnisse der Biologie* **XX**, 1-26.
- Sandberg, P. A. & Plusquellec, P. L. 1969: Structure and polymorphism of normal pores in Cytheracean ostracoda (Crustacean). *J. Paleont.* **43**, 517-521.
- Schmidt, W. J. 1924: *Die Bausteine des Tierkörper in Polarisierendem Licht.* Bonn: Cohen.
- Towe, K. M. & Cifelli, R. 1967: Wall ultrastructure in the calcareous foraminifera: crystallographic aspects and a model for calcification. *Journ. Paleont.* **41**, 742-762.
- Travis, D. F. 1963: Structural features of mineralization from tissue to macromolecular levels of organization in the decapod crustacea. *Ann. N. Y. Acad. Sci.* **109**, 177-245.
- Triebel, E. 1941: Fossile Arten der Ostracoden-Gattung *Paracypredeis* Klie. *Senckenbergiana* **23**, 153-164.
- Triebel, E. 1950: Homeomorphe Ostracoden-Gattungen. *Senckenbergiana* **31**, 313-330.
- Triebel, E. 1956: Brachwasser-Ostracoden von den Galapagos-Inseln. *Senckenbergiana* **37**, 447-467.
- Wood, A. 1949: The structure of the wall of the test in foraminifera; its value in classification. *Quart. Journ. geol. Soc. London* **104**, 229-255.

## Plate 1

Figs 1-2. *Cypredeis* sp.

1: Transmitted light.  $\times 75$ .

2: Transmitted light. Crossed nicols.  $\times 75$ .

Fig. 3. *Xestoleberis* sp. Two-stage replica of etched longitudinal section showing organic membranes enclosing the crystal units and organic sheets. (TEM)  $\times 2000$ .

## Plate 2

Fig. 1. *Xestoleberis* sp. First two-stage replica of transverse section after etching showing concentration of organic membranes and organic sheets. (TEM)  $\times 4000$ .

Fig. 2. *Cypredeis* sp. Fourth two-stage replica of etched longitudinal section. Two-parallel organic sheets run from upper right to lower left. (TEM)  $\times 6000$ .

Fig. 3. *Xestoleberis* sp. Two-stage replica of etched transverse section of the marginal zone. *i*: Inner lamella; *ol*: Outer lamella; *m*: Marginal zone. (TEM)  $\times 2000$ .

## Plate 3

Figs 1-2. *Trachyleberis dunelmensis*

1: Two-stage replica of etched tangential section. The distal part of a spine is seen in transverse section. A pore canal tube is situated near the periphery. (TEM)  $\times 2000$ .

2: Two-stage replica of etched tangential section. The proximal part of a spine is seen in transverse section. The central part consists of few larger crystal units, while they are of normal size in the periphery. (TEM)  $\times 2000$ .

## Plate 4

Figs 1-2. *Cypredeis* sp.

1: One-stage replica of deeply etched specimen showing the organic matrix. The organic membranes have perforations of an order of magnitude of  $0.1 \mu$ . (TEM)  $\times 30000$ .

2: One-stage replica of deeply etched specimen showing the organic matrix. The bright upper area is the formvar carrying film. (TEM)  $\times 2000$ .

## Plate 5

Fig. 1. *Xestoleberis* sp. Broken valve with a normal pore canal viewed from the inner valve surface. *a*: Cone-shaped inner limitation of the pore canal. (SEM)  $\times 5000$ .

Fig. 2. *Xestoleberis* sp. Broken valve with a normal pore canal viewed from the outer valve surface. *op*: Organic pore plate; *s*: Seta which penetrates the centre of the pore plate; *sp*: Small pore tubes. (SEM)  $\times 5000$ .

Fig. 3. *Trachyleberis dunelmensis*. Normal pore canal with a seta penetrating the centre of a spine. (SEM)  $\times 1000$ .

Fig. 4. *Xestoleberis* sp. Edge of etched broken valve. The inner and outer organic layers and the organic matrix remain after etching. (SEM)  $\times$  2000.

#### Plate 6

Fig. 1. *Cythereis* sp. Longitudinal section of a normal pore canal. *op*: Organic pore plate where the perforation are filled by the embedding material. *pt*: Pore tube wall. (SEM)  $\times$  2000.

Fig. 2. *Cythereis* sp. Normal pore canal viewed from the outer surface. *op*: Organic pore plate with perforations. *s*: Seta penetrating the centre of the pore plate. (SEM)  $\times$  5000.

Fig. 3. *Cypreideis* sp. Two-stage replica of etched surface showing a normal pore canal. The outline of the pore plate is heart-shaped. (TEM)  $\times$  3500.

Fig. 4. *Cypreideis* sp. Broken valve showing normal pore canal. *p*: The outer part of the pore canal penetrated by small pore tubes; *s*: Seta; *sc*: The empty seta canal. (SEM)  $\times$  3000.

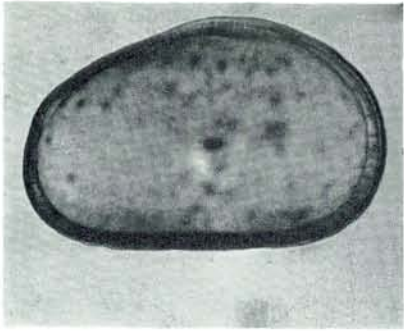
#### Plate 7

Fig. 1. *Bythocypris* sp. Broken valve showing a normal pore canal. *pt*: Pore tube; *ct*: Pore cavity in the distal part filled in with spongy material. (SEM)  $\times$  5000.

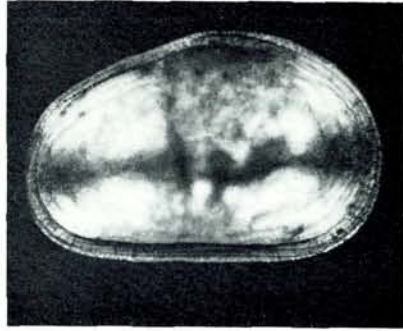
Fig. 2. *Bythocypris* sp. The outer opening of a normal pore canal. (SEM)  $\times$  7500.

Fig. 3. *Cythereis* sp. Marginal pore canals. The valve was broken in the marginal zone. (SEM)  $\times$  1500.

Fig. 4. *Cythereis* sp. Marginal pore canals. The inner lamella was partly broken. *i*: Inner lamella; *mp*: Marginal pore canals; *s*: Seta in the marginal pore canals. (SEM)  $\times$  1000.



1



2



3

10  $\mu$



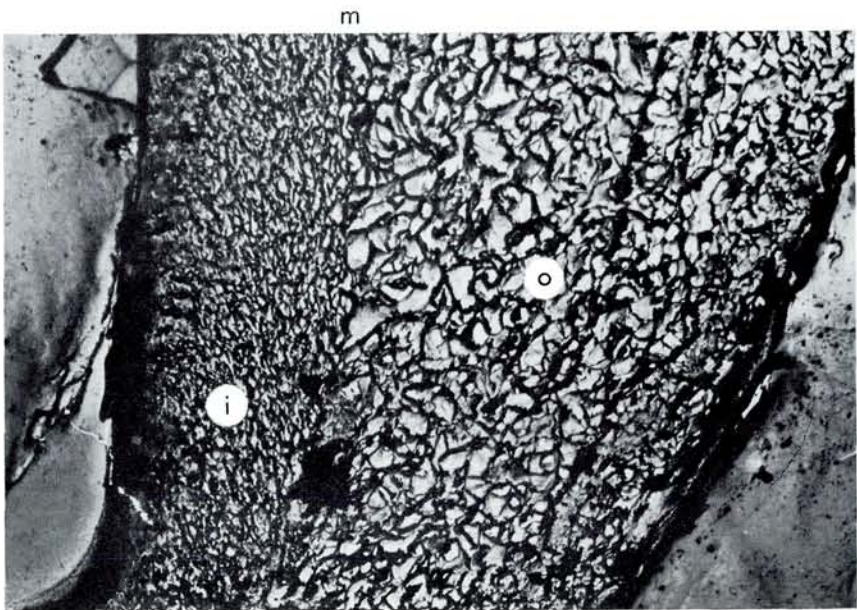
1

5  $\mu$



2

3  $\mu$

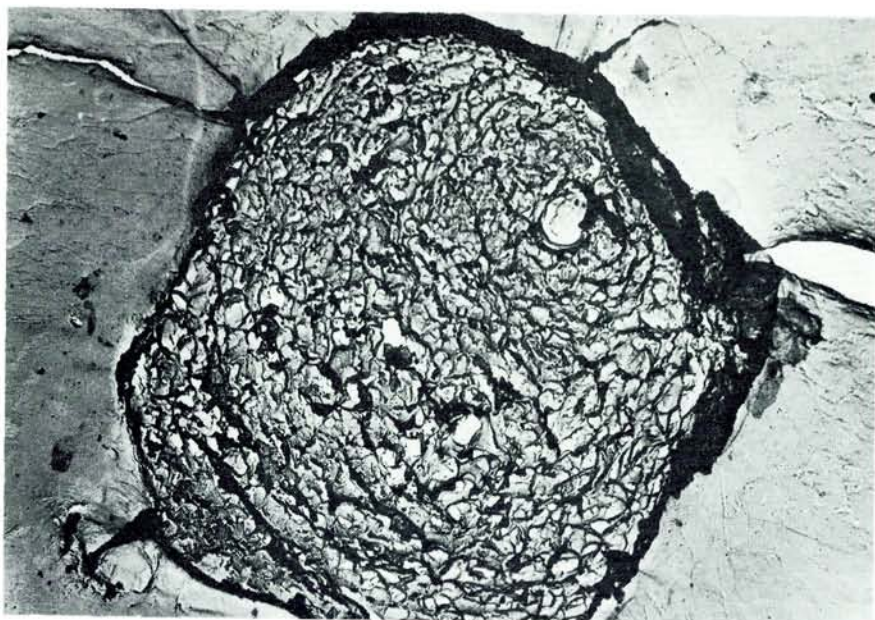


3

m

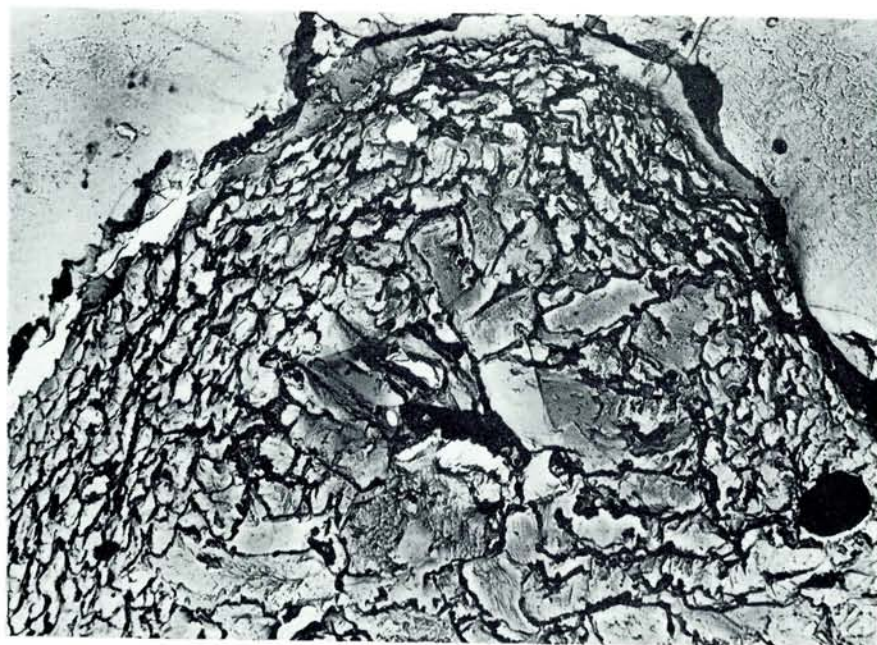
10  $\mu$





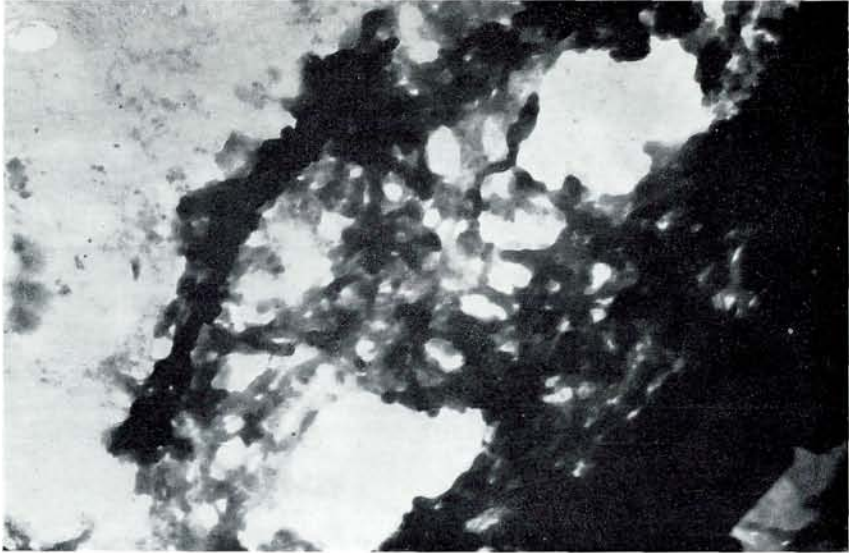
1

10 μ



2

10 μ

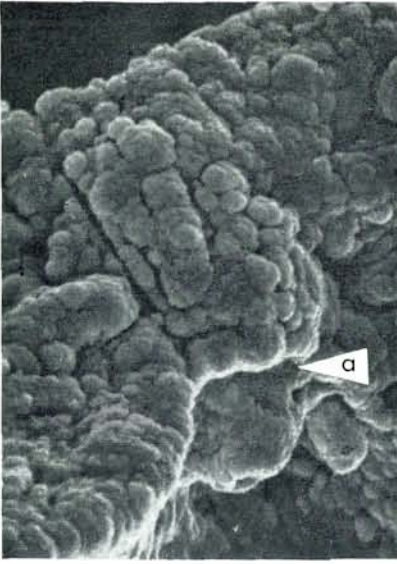


0,5  $\mu$

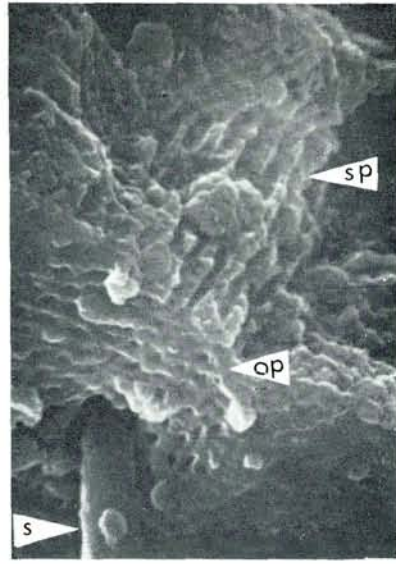


2

10  $\mu$



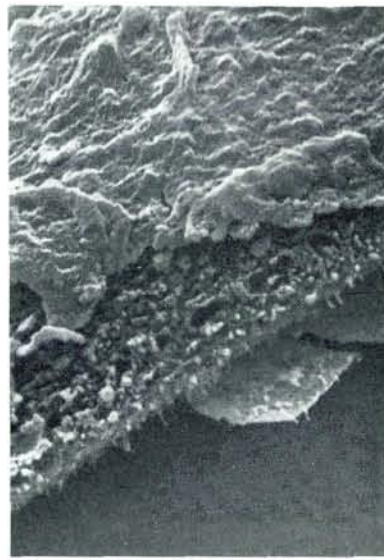
1 4 μ



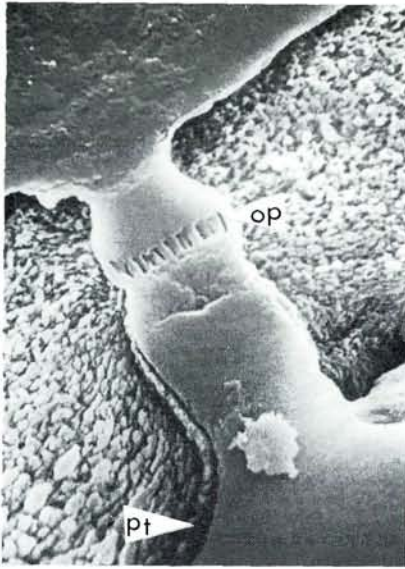
2 4 μ



3 20 μ

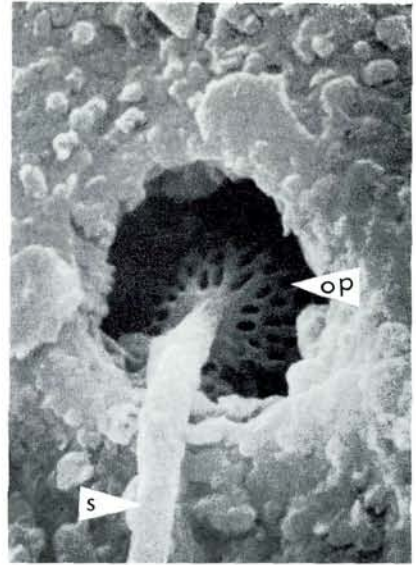


4 10 μ



1

10  $\mu$



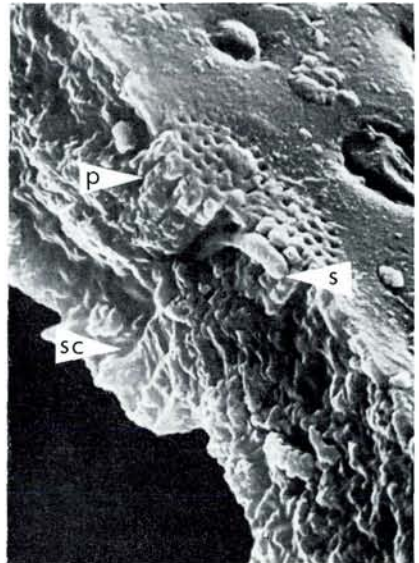
2

4  $\mu$



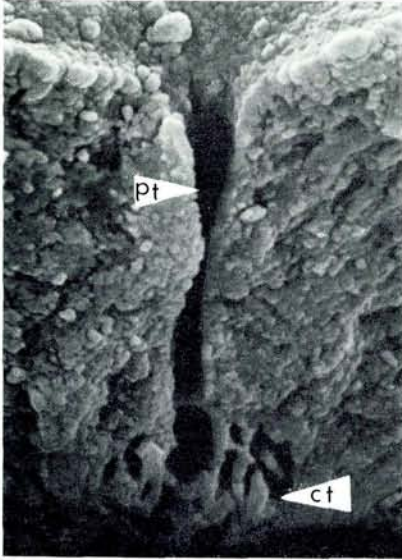
3

6  $\mu$



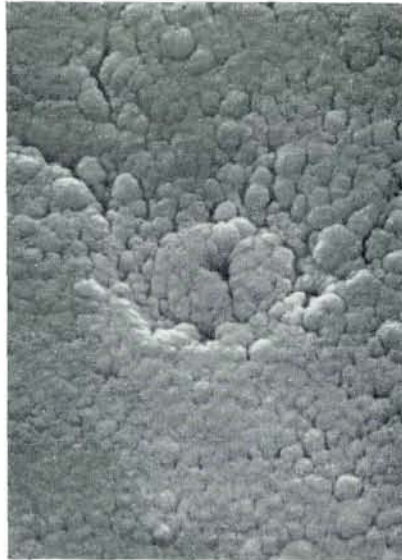
4

7  $\mu$



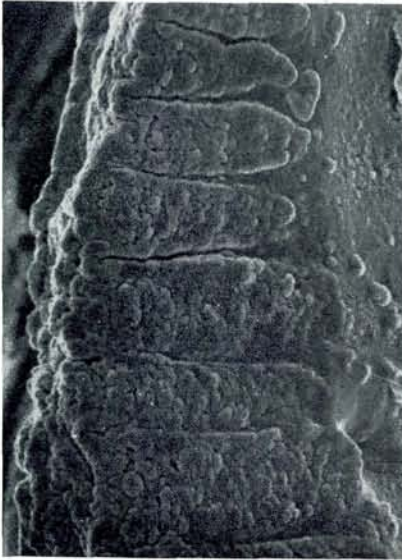
1

4  $\mu$



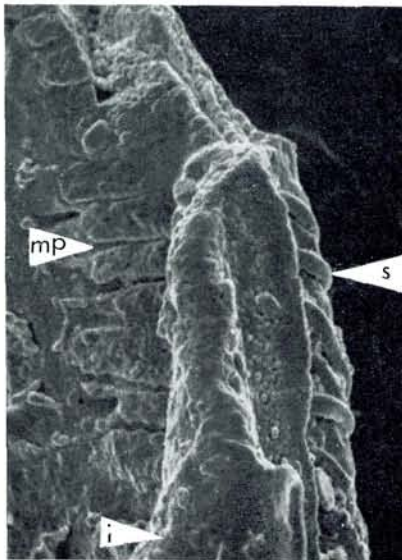
2

2  $\mu$



3

10  $\mu$



4

20  $\mu$